Environmental Research 238 (2023) 116909

Contents lists available at ScienceDirect

Environmental Research

journal homepage: www.elsevier.com/locate/envres

Synthesis and characterization of nanobiochar from rice husk biochar for the removal of safranin and malachite green from water

Sadia Aziz [a], Bushra Uzair [a,**], Muhammad Ishtiaq Ali [b], Sundas Anbreen [a], Fatiha Umber [a], Muneeba Khalid [a], Alaa AA. Aljabali [c], Yachana Mishra [d], Vijay Mishra [e], Ángel Serrano-Aroca [f], Gowhar A. Naikoo [g], Mohamed El-Tanani [h], Shafiul Haque [i,j], Abdulmajeed G. Almutary [k,l], Murtaza M. Tambuwala, MSc.,PhD [m,*]

[a] International Islamic University, Islamabad, Pakistan
[b] Quaid I Azam University, Islamabad, Pakistan
[c] Department of Pharmaceutical Sciences, Yarmouk University, Irbid, Jordan
[d] School of Bioengineering and Biosciences, Lovely Professional University, Phagwara, Punjab, 144411, India
[e] School of Pharmaceutical Sciences, Lovely Professional University, Phagwara, Punjab, 144411, India
[f] Biomaterials and Bioengineering Lab Translational Research Centre San Alberto Magno, Catholic University of Valencia San Vicente Mártir, Valencia, Spain
[g] Department of Mathematics & Sciences, College of Arts & Applied Sciences, Dhofar University, 211, Salalah, Oman
[h] College of Pharmacy, Ras Alkhama Medical and Health Sciences University, United Arab Emirates
[i] Research and Scientific Studies Unit, College of Nursing and Allied Health Sciences, Jazan University, Jazan, 45142, Saudi Arabia
[j] Gilbert and Rose-Marie Chagoury School of Medicine, Lebanese American University, Beirut, 1102 2801, Lebanon
[k] Department of Biomedical Sciences, College of Health Sciences, Abu Dhabi University, Abu Dhabi, 59911, United Arab Emirates
[l] Department of Medical Biotechnology, College of Applied Medical Sciences, Qassim University, 51452 Buraydah, Saudi Arabia
[m] Lincoln Medical School - Universities of Nottingham and Lincoln, University of Lincoln, Brayford Pool, Lincoln, LN6 7TS, Lincolnshire, UK

ARTICLE INFO

Keywords:
Rice husk
Biochar
Nanobiotechnology
Malachite green dye
Safranin dye
Pyrolysis
Adsorption
Dye removal

ABSTRACT

Xenobiotic pollution in environment is a potential risk to marine life, and human health. Nanobiotechnology is an advanced and emerging solution for the removal of environmental pollutants. Adsorption-based technologies are being used to alleviate the global prevalence of xenobiotics like dyes, due to their high efficacy and cost effectiveness. Current study explored the potential of nanobiochar syntehsized via ultrasonication and centrifugation from rice husk for dye removal from water. It involves the synthesis of nanobiochar from rice husk biochar for removal of Safranin, Malachite green, and a mixture of both from aqueous water. Biochar was synthesized through pyrolysis at 600 °C for 2 h. To convert it into nanobiochar, sonication and centrifugation techniques were applied. The yield obtained was 27.5% for biochar and 0.9% for nanobiochar. Nanobiochar analysis through Fourier-Transform Spectrometer (FTIR), X-ray Power Diffraction (XRD) and scanning electron microscopy (SEM) suggested its crystalline nature having minerals rich in silicon, with a cracked and disintegrated carbon structure due to high temperature and processing treatments. Removal of dyes by nanobiochar was evaluated by changing different physical parameters i.e., nanobiochar dose, pH, and temperature. Pseudo-first order model and pseudo-second order model were applied to studying the adsorption kinetics mechanism. Kinetics for adsorption of dyes followed the pseudo-second order model suggesting the removal of dyes by process of chemical sorption. High adsorption was found at a higher concentration of nanobiochar, high temperature, and neutral pH. Maximum elimination percentages of safranin, malachite green, and a mixture of dyes were obtained as 91.7%, 87.5%, and 85% respectively. We conclude that nanobiochar could be a solution for dye removal from aqueous media.

* Corresponding author.
** Corresponding author.
E-mail addresses: sadiaawanqau@gmail.com (S. Aziz), bushra.uzair@iiu.edu.pk (B. Uzair), ishimrl@qau.edu.pk (M.I. Ali), sundusanbreen3@gmail.com (S. Anbreen), fatiha.bsbt1094@iiu.edu.pk (F. Umber), muneebakhalid369@gmail.com (M. Khalid), alaaj@yu.edu.jo (A.AA. Aljabali), vijay.20352@lpu.co.in (V. Mishra), angel.serrano@ucv.es (Á. Serrano-Aroca), gahmed@du.edu.om (G.A. Naikoo), eltanani@rakmhsu.ac.ae (M. El-Tanani), shafiul.haque@hotmail.com (S. Haque), abdulmajeed.almutary@adu.ac.ae (A.G. Almutary), mtambuwala@lincoln.ac.uk (M.M. Tambuwala).

https://doi.org/10.1016/j.envres.2023.116909
Received 3 July 2023; Received in revised form 8 August 2023; Accepted 16 August 2023
Available online 4 September 2023

1. Introduction

All life depends on the water on Earth. The quality of water is deteriorating due to anthropogenic activities including massive release of xenobiotics directly into water bodies (Vishnu et al., 2022). Xenobiotics are manmade compounds covering variety of pollutants and contaminants. Xenobiotics like dyes are the second major cause of water pollution. Dyes are very complex organic substances, having vast applications in various fields of life (Benkhaya et al., 2020). Until the late-twentieth century, dyes were produced from natural materials like plants, minerals, and animals being less toxic and biodegradable. With the growth of industrialization, synthetic dyes are being produced to meet industry demand with almost 8 thousand registered chemically produced dyes in Color Index (C.I.) (Yuan et al., 2020a).

The dyes are categorized into various classes such as azoic, basic, acid, direct, onium, disperse, metallic, oxidative, pigment, mordant, reactive, solvent, vat, and sulphur dyes (Vigneshwaran et al., 2021). Safranin and malachite green are the dyes having extensive applications in textile industry for dyeing leather, silk, wool etc, but have severe draw backs in terms of their impacts on human health causing skin and respiratory tract irritation, leading to permanent damage to the cornea and conjunctiva (Vigneshwaran et al., 2021) lesions on skin, vomiting, and haemorrhage (Eltaweil et al., 2020).

Conventional chemical and physical methods applied to remove xenobiotics are time-consuming, costly, and are sophisticated in design, while biological treatment systems required a controlled environments (Heidarinejad et al., 2020). In recent years, employment of biochar for the removal of pollutants is gaining attention. Biochar is enriched in carbon-containing substances obtained from pyrolysis of biological waste in the absence of oxygen with vast applications of removal of contaminants, soil improvement, microbial growth, and increasing plant biomass (Pan et al., 2021). Biochar is an eco-friendly, cost-effective, and efficient adsorbent due to its high specific area, high porosity, and high pore volume (Chen et al., 2021). Different methods are utilized to activate it or enhance its adsorption capabilities like the addition of acid, metal impregnation, and further fabrication techniques. In a study bamboo charcoal (BC) was used as a filler to modify polyurethane (PU) foam forming BC/PU foam composite for removal of organic solvents from waste water. Results revealed BC-loaded PU (BC/PU) foam composites effectively removed seven organic solvents from water (Wang et al., 2022a). In another study metal loaded multi walled carbon nanotubes were found to be effective adsorbent to remove nitrate form aqueous solution (Wang et al., 2021). In a dye removal study a composite of stalk BC (SBC) and nanoscale zero-valent iron (nZVI) was biosynthesized which effectively removed dye from aqeous solution. The composite displayed a synergetic role in enhancing dye removal (Liu et al., 2022). In a similar study, pulp sludge derived biochar was modified via $ZnCl_2$ and applied to effectively remove methylene blue (MB) from aqueous solutions with maximum removal in first 24 h (Zhao et al., 2021).

In the domain of biochar, Nanobiochar is an advanced technique in removal studies, as it has overcome many limitations come across while applying only biochar, as multiple functions of biochar were restricted due to limited surface functionalities. Application of nanotechnology by reducing biochar to a nano-sized range and binding multiple functional groups resulted in increased adsorption capacity with mechanical and thermal stability (Noreen and Abd-Elsalam, 2021). Reactive organic species (ROS) produced by an increase in negative zeta potential, reduction in hydrodynamic radius, and increase in oxygen and carbon-containing functional groups of nanobiochar upgrades its adsorption capacity (Ramanayaka et al., 2020a,b). With its surface hydrophobicity, nano-scale size, high specific surface area, and micro-porous structure, nano-BC possesses enhanced adsorption and immobilization capabilities for a wide array of pollutants, including heavy metals, pesticides, PCBs, PAHs, and more (Chauhan et al., 2023; Naseri et al., 2023). The presence of diverse surface functionalities such as hydroxyl, carboxy, and lactonyl groups further augments its pollutant removal efficiency. In addition, nano-BC has proven to be an excellent immobilization material for enzymes, effectively functioning as a nanocatalyst (Syed et al., 2023). Researchers also have successfully developed nano-BC supported photocatalysts using various methods, which exhibit remarkable potential in the photocatalytic breakdown of water pollutants (Ramasundaram et al., 2023; Subramanian et al., 2023). Nanobiochar has also found its applications in medicine as nanocarrier for targeted drug delivery (Saadh et al., 2023).

In recent times, the electrochemical characteristics of nano-BC have attracted attention due to its potential as an alternative to carbon electrodes. Its high adsorption capacity allows for selective entrapment of chemicals, leading to improved chemical concentration on the electrode surface and enhanced sensitivity in electrochemical biosensors for detection purposes (Karimi-Maleh et al., 2023).

Beyond its role in adsorptive removal and optoelectronic applications, nano-BC has also been explored for energy storage (Oliveira et al., 2023; Aarimuthu et al., 2023). Moreover, it has been tested for other innovative uses, including being used as a material for solid fuel briquettes to produce pellet biofuels and in the formulation of bio-fertilizers (Chauhan et al., 2023; Heshammuddin et al., 2023).

Data on the applications of nanobiocahr is limited however nanobiochar has great adsorption capability for several pollutants like dyes, antibiotics, herbicides, polychlorinated biphenyls (PCBs), heavy metals, and polycyclic aromatic hydrocarbons (PAH) owing to their surface hydrophobicity, large specific surface area, and micro porosity. Synthesis methodology and type of feedstock material have a major impact on the properties and characteristics of nanobiochar (Rajput et al., 2022). Nanobiochar has garnered considerable attention for its diverse applications in various fields, such as biosensors, soil amendments, and photocatalytic materials. However, its potential in water treatment is little explored. Most of the current nanobiochar production relies on the Ball milling method, with limited attention given to the use of ultrasonication technology—a safe and effective approach to produce nanobiochar from bulk biochar.

In this study, we propose investigating the application of rice husk nanobiochar, derived via the sonication and centrifugation method, for the removal of dyes (malachite green and safranin) from water. Despite the significant advancements in nanobiochar research, data on its efficiency in dye removal through this particular approach is currently lacking. By exploring the potential of nanobiochar in water treatment, we aim to contribute valuable insights to the field. The utilization of ultrasonication technology in nanobiochar production offers a promising avenue for sustainable and efficient synthesis.

Current study investigated the physiochemical characteristics of nanobiochar and its application for adsorption and removal of dyes from aqueous solution under different conditions and parameters. It also presents an overview of impact of varying factors on removal rate of dyes by nanobiochar following different kinetic models.

2. Materials and methods

2.1. Materials

In this study rice husk was used as a substrate to prepare biochar. Rice husk was bought from local market Sialkot, Pakistan. Dyes selected for removal study were malachite green, and safranin purchased from Sigma-Aldrich company. Filter paper (Wattman), beakers (500 ml), Conical Erlenmeyer flask, distilled water, hydrochloric acid, UV visible spectrophotometer (Agilent 8453, 2005, PerkinElmer, 2010), Teflon Magnetic Stirrer, Digital Weighting Balance, Thermometer, pH meter, EC meter, Automatic shaker set at 37 °C, Sonicator (Sweep Zone technology, USA), Micropipette, Centrifuge (B. Bran, Germany), and distillator were the materials and instruments used throughout the study.

2.2. Preparation of biochar

Biochar was produced by the process of pyrolysis (Sarkar et al., 2019). Rice husk was washed with distilled water, dried in the open air and subjected to pyrolysis at 600 °C for 2 h in a muffle furnace.

2.3. Synthesis of nanobiochar

Nano biochar was prepared according to previous work (Song et al., 2019). Biochar was ground in mortar and pestle. Finely grounded 10 g of biochar was added to 400 ml of distilled water. The solution was stirred for 2 min on the magnetic stirrer. Sonicated for 30 min and stirred again for 5 min. The mixture was kept overnight for the particle size of less than 1 μm (<1 μm) to settle down according to Strokes Law. The upper layer was collected and centrifuged for 30 min at a speed of 3500 rpm. The supernatant was collected in petri plates and dried in a desiccator at 37 °C. After drying dried layer of nanobiochar was scratched by a scratcher and collected in an Eppendorf tube (Fig. 1).

2.4. Biochar and nanobiochar characterization

The yield of biochar was found by the formula:

$$\text{Yield\%} = \frac{\text{weight of rice husk before pyrolysis}}{\text{weight of rice husk after pyrolysis}} \times 100$$

The yield of nanobiochar was found by the formula:

$$\text{Yield\%} = \frac{\text{Mass of nanobiochar}}{\text{mass of biochar}} \times 100$$

Biochar and nanobiochar were characterized by the following characterization techniques: pH and EC of both biochar and nanobiochar were determined in 1:10 (w/v) sample-to-water ratio as described by (Singh et al., 2017). FTIR spectra of both biochar and nanobiochar samples were obtained with (FT-IR, PerkinElmer, 2012) FTIR spectrophotometer in the wavelength range of 4000–550 cm^{-1}. X-ray powder diffraction (XRD, PANAINTICAL, 2006 Wax.) was performed by monochromatic X-ray radiations of wavelength 1.542 Å, scan in the range of 10–60° (2θ), and scan at the speed of 2° per min for both samples. Surface morphology of biochar and nanobiochar was observed using a JSM 5910 lv thermionic scanning electron microscope (Jeol SEM, Japan) to establish macro-pore shape.

2.4.1. Experimental set up

Safranin dye (Basic dye, Chemical formula: C20H19ClN4, and Molar mass 350.85 g/mol), malachite green (Basic dye, Molar mass: 364.911 g/mol, Chemical formula: C23H25ClN2). For adsorption purposes, 2 mg of safranin, malachite green, and a mixture of both dyes were dissolved in 100 ml of distilled water in 3 different Erlenmeyer flasks. Solutions were stirred for 5 min. Nanobiochar was added to each flask. Mixtures were kept in a shaker at room temperature for 2.5 h 2 ml of the mixture was withdrawn from each flask at (0 min, 30 min, 60 min, 90 min, 120 min, and 150 min). An aliquot was filtered and analysed for dye removal at wavelength 617 nm for malachite green and 519 nm for safranin by UV visible spectrophotometer.

Different variables were used to measure the effect of the different parameters on the adsorption potential of nanobiochar. These parameters are following.

2.4.2. pH effect on the removal of dyes

NaOH and H_2SO_4 solutions of amounts 1, 0.1, and 0.01 mol/L were used to adjust the pH at 7 and 9. For that 2 mg of safranin, malachite green, and mixed dyes were added to 100 ml of distilled water. 20 mg nanobiochar was kept constant for both pH values. Solutions were stirred for 5 min and placed in a shaker. Aliquots were withdrawn after every half an hour for about 2.5 h. Samples were filtered and observed via UV spectroscopy to check absorbance at respective wavelengths.

2.4.3. Nanobiochar dose effect on the removal of dyes

For studying the effect of nanobiochar dose 2 mg of safranin, malachite green, and mixed dyes were added to 100 ml of distilled water at two different concentrations of nanobiochar i-e 10 mg and 20 mg. Solutions were stirred for 5 min and placed in a shaker. Aliquots were withdrawn after every half an hour for about 2.5 h. Samples were filtered and observed via UV spectroscopy to check absorbance at respective wavelengths.

2.4.4. Study of temperature effect on the removal of dyes

To measure the effect of temperature 2 mg of safranin, malachite green, and a mixture of both dyes was dissolved in 100 ml of distilled water in 3 different Erlenmeyer flasks. Solutions were stirred for 5 min 20 ml nanobiochar was added to each flask. Mixtures were kept in a shaker at two temperatures 35 °C and 50 °C for 2.5 h. Aliquots were withdrawn after every half an hour for about 2.5 h. After filtration,

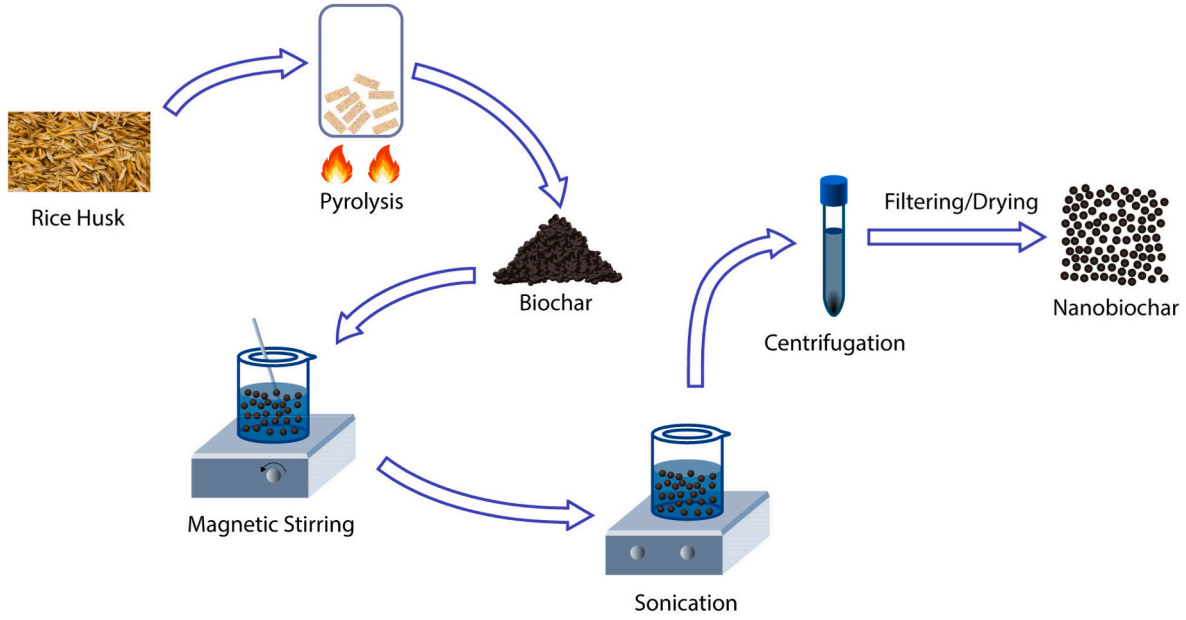

Fig. 1. Nanobiochar preparation from Rice husk.

filtrates that were left with residual concentrations of respective dyes were subjected to UV spectroscopy to measure the absorbance values (Table 1).

The two Adsorption Kinetic models i.e. Pseudo First order and Second order were applied, analysed, and calculated for the adsorption kinetics of the malachite green, safranin, and mixture of dye uptake by nanobiochar and to evaluate adsorption mechanisms.

2.4.4.1. Statistical analysis. All experiments were run in duplicate and data was statistically analysed by calculating arithmetic mean and standard deviation. Microsoft excel and origin were used to analyze data and plot graphs.

3. Results

3.1. The yield of biochar and nanobiochar

The yield of biochar obtained was 27.16% and of nanobiochar it was 0.9%. The yield of biochar is affected by two factors i.e., pyrolysis temperature and time. As temperature increases yield decreases, this is due to aromatization, dehydrogenation, decarboxylation, deoxygenation, and dehydration at a higher temperature that resulted in enhanced carbonization (Nwajiaku et al., 2018). Similarly, longer the time of pyrolysis leads to more evaporation of volatile components which reduces the yield. In the case of rice husk, it contains lignin and cellulose, pyrolysis causes carbonization of lignin with reduction of hydrogen and oxygen releasing volatile organic compounds and carbon dioxide. Increase in temperature induce conversion of O-alkyl C to aryl and O-aryl furan like structures which are chemically very active (Yang et al., 2019). Pectin and lignin components reduce by increasing pyrolyis temperature as described in FTIR spectra. Pyrolysis at high temperatures shows yields in the range of 20%–30% (Bushra and Remya, 2020). Physiochemical properties of nanobiochar are influenced by the composition of the raw material used. Previous studies have indicated that biomass with high hemicellulose content tends to yield nanobiochar with low carbon content and high oxygen content (Weber and Quicker, 2018). The yield of nano-biochar is primarily affected by the oxygen-to-carbon (O/C) molecular ratio during pyrolysis and the ash content. A higher O/C ratio in the feed substrate reduces the selectivity of nano-biochar and increases bio-oil formation, whereas a lower ash content leads to higher nano-biochar yield and reduced bio-oil yield (Goswami et al., 2022).

Rice husk, which is rich in cellulose and hemicellulose, has a high O/C ratio, influencing the ash content and overall yield of nanobiochar compared to bulk biochar. Notably, the ash content increases as particle sizes decrease, from feedstock to bulk biochar to nanobiochars, which aligns with previous reports (Qian et al., 2016). This trend is particularly evident in biochar produced from plant biomass sources such as wood, herbs, and agricultural waste, where ash content increases significantly with decreasing particle sizes (NP > MP > Bulk). For instance, wood chip bulk biochar had an ash content of 5.73%, while MP biochar increased to 13.5% and NP biochar reached 43.4%. This phenomenon is attributed to the accumulation of inorganic salts and hydrated ions during extraction (Song et al., 2019). Moreover, the ash content of nanobiochar produced from agricultural waste is directly proportional to the bulk biochar, but it varies depending on the type of crop residues. For instance, corn straw nanobiochar has a lower ash content than rice straw nanobiochar, mainly due to rice straw containing more silicon (Si) than corn straw (Ma et al., 2019).

In addition to the raw material, the pyrolysis temperature also influences the ash content (Anupama and Khare, 2021). With increasing pyrolysis temperature, the base cation and carbonate content of biochar increase, resulting in higher total ash content (Ramanayaka et al., 2020a,b). For example, the ash content of sugarcane bagasse biochar at 800 °C was 2–3 times higher than that of low-temperature biochar (Jiang et al., 2023). Furthermore, ultrasonic nanobiochar has significantly lower ash content compared to pristine biochar, with approximately a 50% reduction due to the separation or dissolution of minerals by the ultrasonic process (Jiang et al., 2023). Conversely, wet milling increases the surface functional groups and ash content of resulting nanobiochars but demonstrates a significant decrease in yield and carbon content (Yuan et al., 2020b).

The yield of nanobiochar from bulk biochar is influenced by two crucial factors: the feedstock and the preparation process. Various techniques, such as ball milling, ultrasonication, and chemical treatments, are applied for nanobiochar production, each having its advantages and limitations, including long duration, high energy and time consumption, or the use of hazardous chemicals (Ng et al., 2022). The physiochemical properties of nanobiochar, such as surface morphology, surface chemistry, and pore size, vary depending on the technique used. Ultrasonication positively affects the specific surface area of carbon from biomass by opening clogged pores and exfoliating the carbon structure, resulting in increased microporous regions and the production of nano-biochar. However, ultrasonication has no noticeable effect on the elemental composition or oxygen-containing functional groups on the biochar's surface. On the other hand, chemical modification aims to alter the functional groups on the material's surface (Wang et al., 2022b).

Therefore, the selection of feedstock and preparatory methods for nanobiochar production should be tailored to the specific application, either using individual techniques or a combination with suitable modifications. This approach ensures the attainment of nanobiochar with a high yield and enhanced physiochemical properties, all while maintaining its optimal performance for the intended purpose.

Table 1
Variables used in the study.

Variables	Change in values
PH	7 and 9
Temperature	35 °C and 50 °C
Concentration of nanobiochar	10 mg and 20 mg

3.2. Characterization

3.2.1. pH and electrical conductivity

pH and EC were measured by pH meter and EC meter respectively. The pH of biochar was recorded 9.1 and the pH of nanobiochar was recorded 8.38. For both biochar and nanobiochar ph. was basic. EC of biochar was 8.8 and nanobiochar 21.5 was recorded. The increase in ash content with increasing temperature increases pH and EC value. Loss of volatile matters and less amount of pectin, cellulose, lignin, hemicellulose, and phenolic compounds contribute toward higher pH values (Vieira et al., 2020). At low temperatures due to more unstable organic carbon and other volatile compounds pH and EC values are low (Mohammed et al., 2021; Vieira et al., 2020)). The EC and pH of the biochar produced from rice husk showed an increasing trend with an increase in pyrolysis temperature as increased pyrolytic temperatures resulted in synthesis of biochar wit high pH (Novak et al., 2009). This is also due to the increase of silicon content with an increase in temperature. In addition, the minerals, carbonates, and inorganic alkalis (such as K and Na), negatively charged surface functional groups also play role in making biochar alkaline. There are variations in nanobiochar and biochar EC and pH values which is due to variation in the concentration of compounds present in both compounds as determined by extra peaks in FTIR spectra. Readings were in accordance with the literature (Monica Nwajiaku et al., 2018).

3.2.2. FTIR

FTIR spectra were recorded in the 515–4000 cm^{-1} region with a resolution of 1 cm^{-1}. Spectra of biochar and nanobiochar represent alkane C–H stretching at (3000–2840 cm^{-1}), 1650–1550 cm^{-1} represent

secondary N–H bend, 1440–1400 cm^{-1} methyl C–H asymmetric stretching, 1085–1050 cm^{-1} primary alcohol C–O stretching, 840–790 cm^{-1} trisubstituted alkene C=C bending and at 795 cm^{-1} C–H bending were found. At 1000–625 cm^{-1} substituent of aromatic rings was found (Song et al., 2019). Additional inorganic components such as sulphates and silicates can also contribute to the broad and intensive peak at 1200–970 cm^{-1}. FTIR spectra analysis shows two peaks between 980 and 1100 cm^{-1} and between 650 and 800 cm^{-1}. These peaks reveal the presence of Si–O–Si bonds with curvature and stretching vibrations. FTIR spectra show less amount of pectin, hemicellulose, and cellulose which are linked with vibrations of the –OH group at 3800 cm^{-1}. The absence of these compounds is due to dehydration of the rice husk as pyrolysis temperature increases (Cantrell et al., 2012; Claoston et al., 2014; Ramanayaka et al., 2020; Vieira et al., 2020) (Fig. 2).

Nanobiochar and biochar have the same peaks but the peaks of nanobiochar were more intense and contain more functional groups with various newly emerging peaks like primary alcohol stretching and aliphatic chains compared with biochar. Agriculture-based biochar with COOH and other CO functional groups offers sorption sites for heavy metals, dyes, and other containment in the environment. FTIR spectrum was following as reported in the literature (Song et al., 2019).

3.2.3. XRD analysis

The XRD pattern is a main broad peak in the low angle region (10°–35°) is index silicone can be present in form of disordered cristobalite (SiO_2) (Morales et al., 2021). Biochar confirmed the presence of amorphous silica as indicated by the heap at 2θ ~ 22.8 due to amorphous silica and quartz, which is a major constituent of these biomaterials (Pottmaier et al., 2013). The diffraction peak at 2Θ = 22–28° shows the presence of carbon structures because at high temperatures the carbon content of bio-char condenses (Amen et al., 2020) (Fig. 3).

It was found that nanobiochar has a sharp diffraction peak at 22.8125° ascribed to the peak of crystalline cristobalite, SiO_2 (Ramanayaka et al., 2020). Stronger peak signals for calcite (CaCO3) (29.3°) were detected. The structure of calcite was well-crystallized (Song et al., 2019). Strong peaks were observed at 2θ = 26.13°, 28.08°, and 29.5° depicting the presence of graphite. A high peak at 2Θ = 24° is a representative of carbon (C_{12} to C_{60}). Compared to biochar, intense and strong peaks in nanobiochar suggested its nanosized crystalline structure (Yue et al., 2019).

3.2.4. SEM analysis

In any adsorption study surface and pore structures of an adsorbent are important features. Surface morphology of rice husk biochar when analysed by SEM showed properly arranged well developed porous structure with visible cracks and shrinkages as discussed by (Claoston et al., 2014). Pyrolyzed structure contains both macro and micropores reflecting high surface area and adsorption capability. The porous structure of rice husk biochar is more regular and compact as the lignin in rice husk was also pyrolyzed alongwith hemicellulose indicating well developed porous structure as studied by (Zhang et al., 2020). Rice husk biochar maintain its intact structure with uniform development of pores in series having capillary structure as reported by (Le et al., 2021). Looking at surface morphology of rice husk nano biochar, the SEM images showed cracked and disintegrated structures with scattered fragments, pore collapse and destructed carbon matrix due to high temperature and processing treatment i.e., grinding, sonication and centrifugation to convert biochar into nanobiochar (Liu et al., 2018) (Fig. 4).

3.3. Adsorption of dyes by nanobiochar

The elimination of safranin, malachite green, and a mixture of dyes had been calculated by using the following formula:

$$\%E = \frac{C_o - C_e}{C_o} \times 100 \quad (1)$$

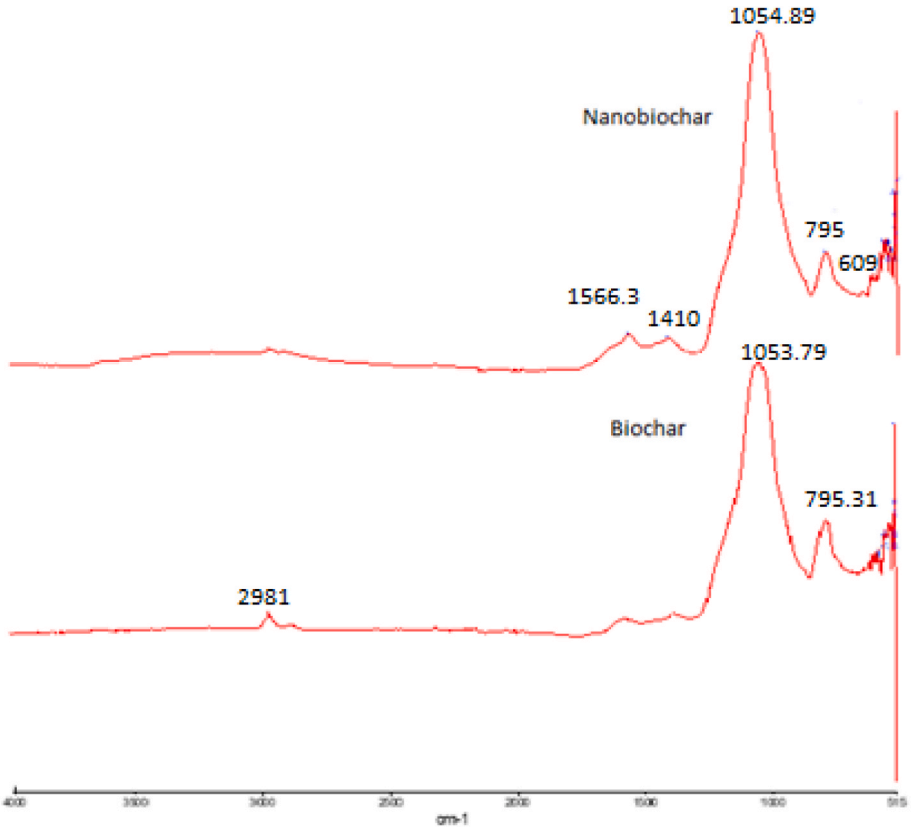

Fig. 2. FTIR spectra of biochar and nanobiochar.

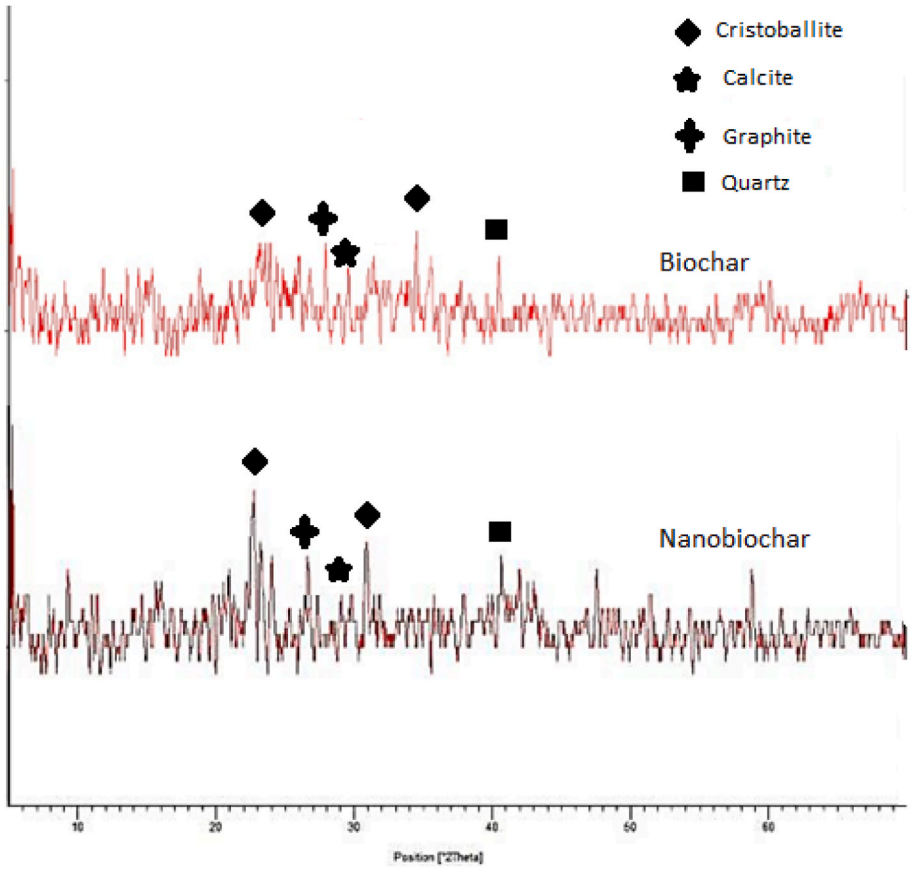

Fig. 3. XRD spectra of biochar and nanobiochar.

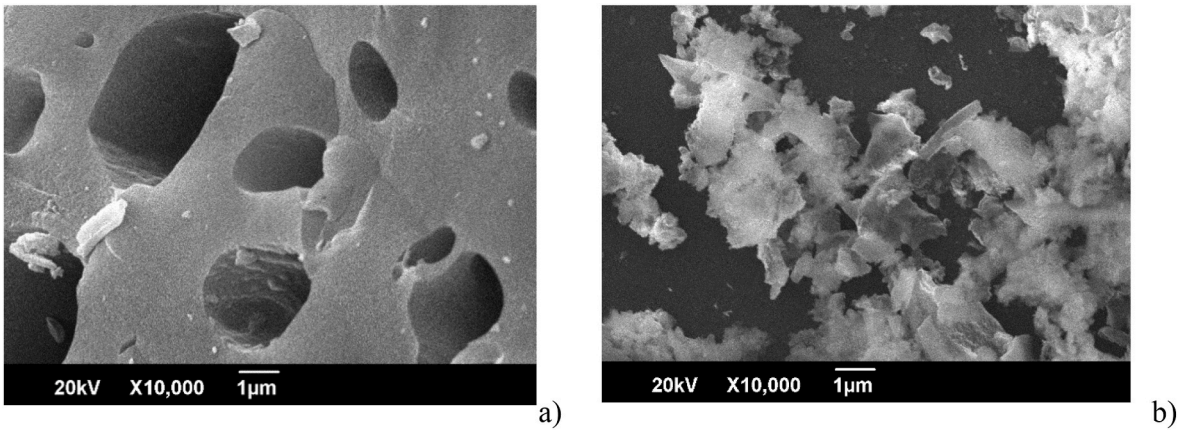

Fig. 4. SEM image of a) biochar and b) nanobiochar.

In Equation (1), Co and Ce refer to initial and final dyes concentrations respectively.

The amount of eliminated dye by nanobiochar at equilibrium was determined by following formula:

$$q_e = \frac{C_o - C_e}{W/V} \quad (2)$$

In Equation (2), Co and Ce refer to initial and final dye concentrations respectively; V is dye volume in liter and W is the mass of biochar in grams.

3.3.1. Study of pH effect on the removal of dyes

For evaluation of the impact of pH on the removal of dyes, the adsorption process was performed under pH7 and pH 9. Elimination percentages of safranin, malachite green, and mixture were 90.8%, 75.9%, and 56.6% respectively at pH 7. While, at pH 9, elimination percentages of safranin, malachite green, and mixture were 80.7%, 58%, and 76%. PH 7 showed favourable results for dyes adsorption separately. Adsorption of the mixture of dyes was high at pH 9 (Fig. 5).

Qt/t graph shows maximum adsorption within 30 min, and then it showed a linear slope. The mixture showed more adsorption at pH 9 than at pH 7 (Fig. 6).

3.3.2. Study of temperature effect on the removal of dyes

For estimation of the impact of temperature on adsorption of dyes, adsorption was done at 35 °C and 50 °C. The elimination percentages of

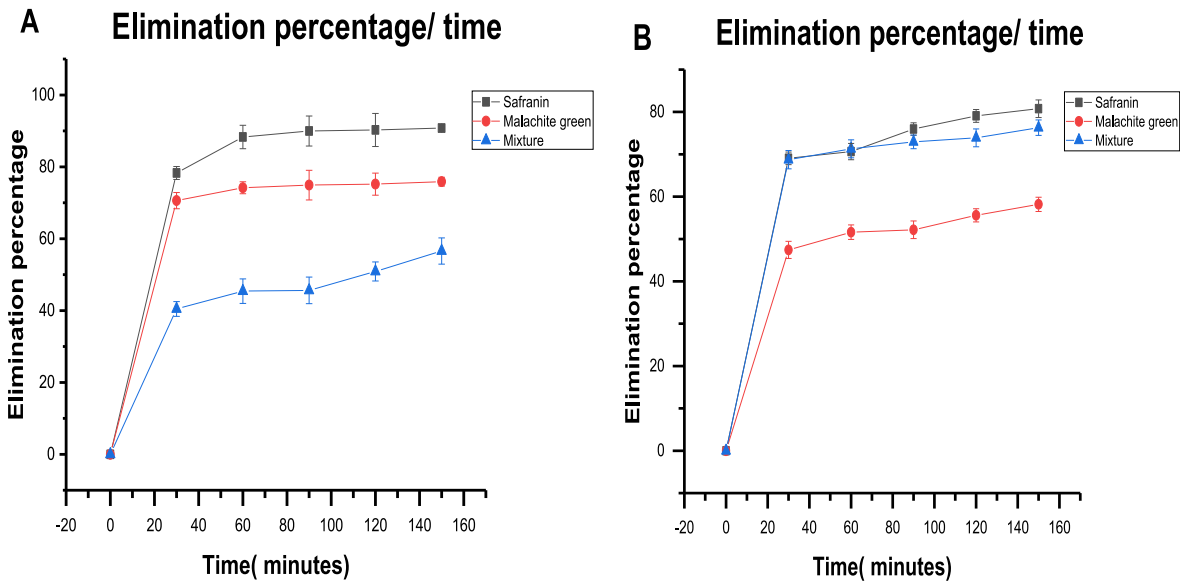

Fig. 5. Effect of pH on removal of dyes (A) pH 7 (B) pH 9.

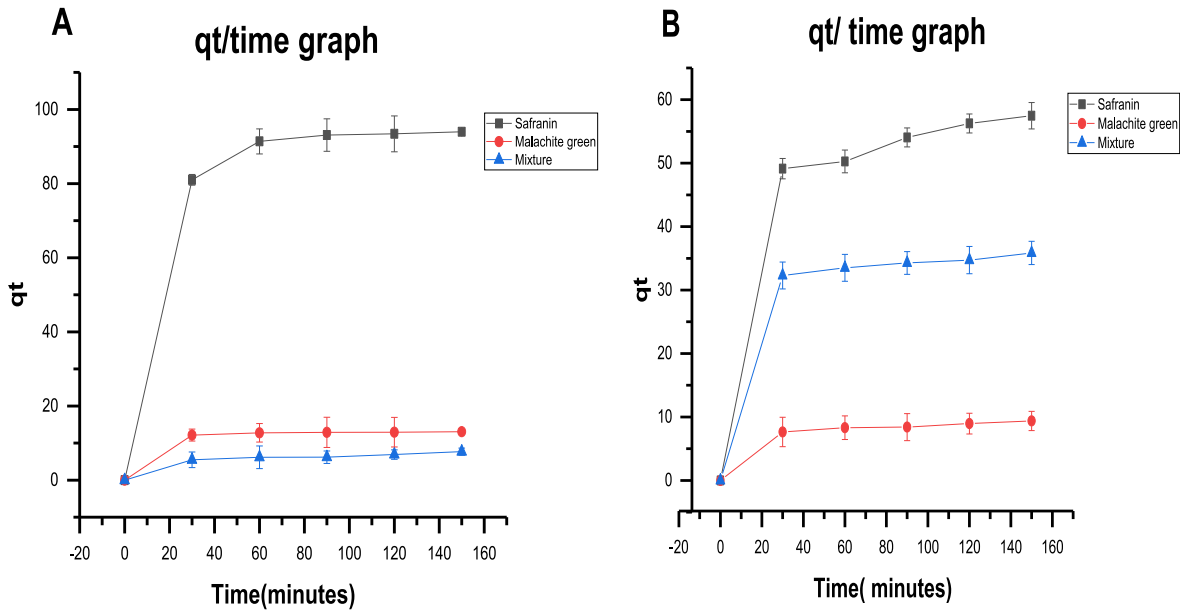

Fig. 6. Plot of qt versus t at pH 7 (A) and pH 9 (B).

safranin, malachite green, and mixture at 35 °C were 90.8%, 75.8%, and 56.6% respectively. Their elimination percentages at 50 °C were 91.7%, 87.5%, and 59.4% respectively. This has shown that adsorption is maximum at high temperatures and 50 °C is the favourable temperature for removal of the dyes (Figs. 7 and 8).

3.3.3. *Study of nanobiochar dose effect on the removal of dyes*

For the judgment of the impact of nanobiochar dose on adsorption, 10 mg nanobiochar and 20 mg nanobiochar were used. The elimination percentages of safranin, malachite green, and mixture were 90.8%, 75.8%, and 56.6% respectively by use of 20 mg nanobiochar. The elimination percentages of dyes by using 10 mg nanobiochar were 86.6%, 68%, and 85.8% respectively. Elimination of safranin, malachite green, and mixture were elevated by an increase in nanobiochar dose (Fig. 9).

Qt versus t graphs showed maximum adsorption of dyes within half an hour. After that, adsorption reached its equilibrium value eventually. A high concentration of safranin dyes had been adsorbed (Fig. 10).

3.4. *Adsorption kinetics*

The kinetic adsorption mechanism process was studied by applying the pseudo-first order model and pseudo-second order model mechanism for data analysis. Pseudo-first order model and pseudo-second order model were done by using linear equations and plots in Table 2. The pseudo-first-order model follows that the rate of adsorption of adsorbate on any adsorbent is proportional to the number of active sites present on the adsorbent while Pseudo-second-order kinetics results from the phenomena of chemisorption.

3.4.1. *Pseudo-first order model*

Pseudo-first order model had been applied to study the adsorption kinetics mechanism. R^2 values for safranin, malachite green, and mixture at 10 mg nanobiochar dose were 0.91357, 0.70727, and

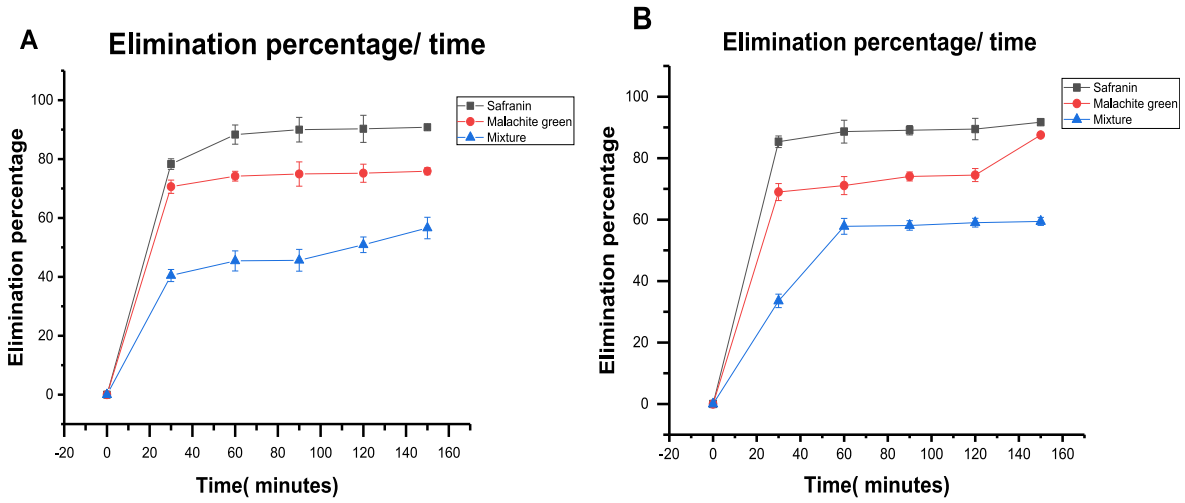

Fig. 7. Effect of temperature on the removal of dyes (A) 35 °C (B) 50 °C qt versus time graph has shown a similar pattern that high adsorption happens within the first 30 min and then the slope becomes linear.

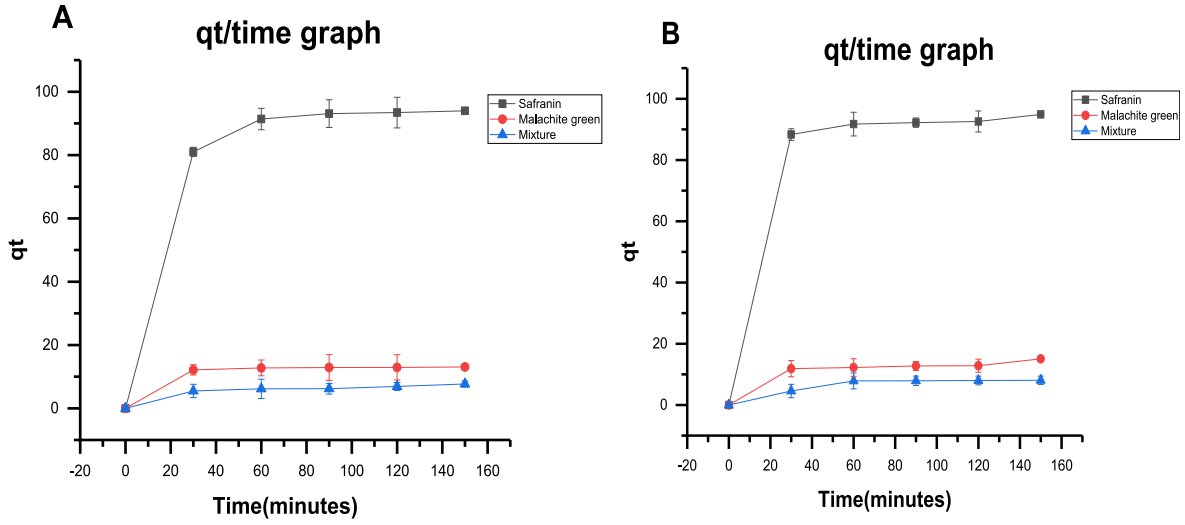

Fig. 8. Plot of qt versus t at temperature A) 35 °C (B) 50 °C.

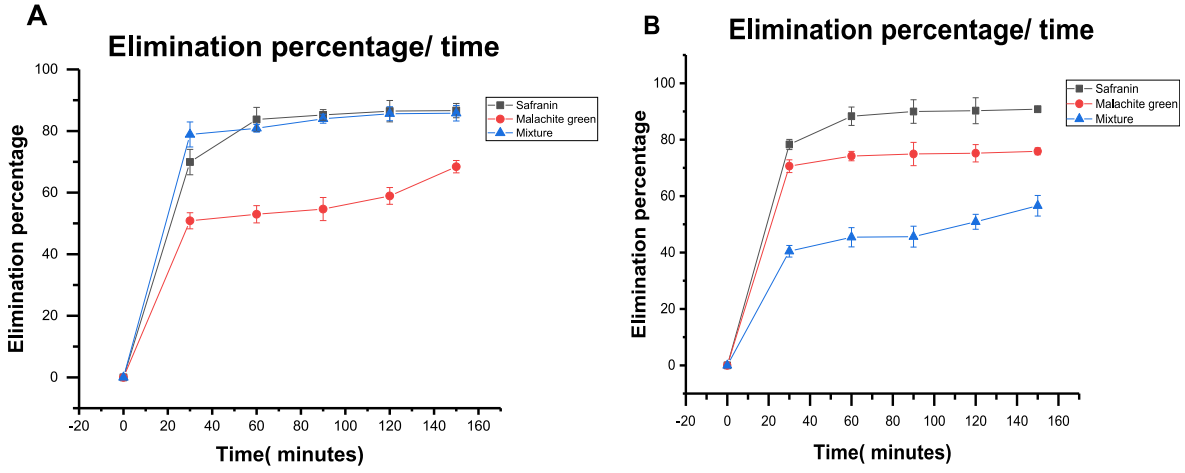

Fig. 9. Effect of nanobiochar dose on the elimination of dyes (A) 10 mg and (B) 20 mg.

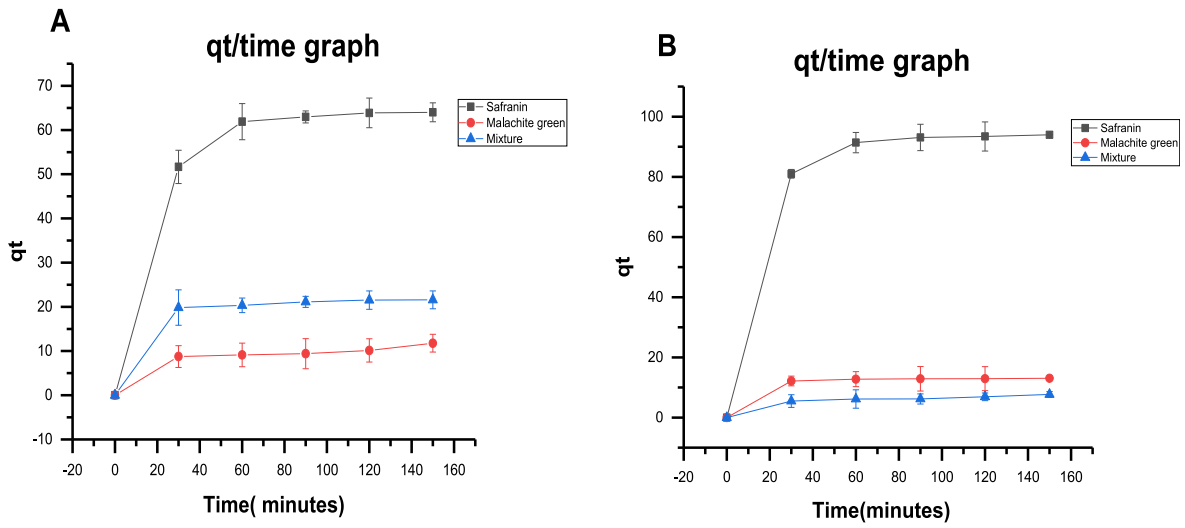

Fig. 10. Plot of qt versus t with (A) 10 mg nanobiochar and (B) 20 mg nanobiochar.

Table 2
Kinetic models applied for evaluation of elimination of dyes.

Kinetic model	Linear equation	Plot
Pseudo-first order model	$ln\,(q_e - q_t) = ln\,q_e - k_1 \times t$	$ln\,(q_e - q_t)$ versus time (t)
Pseudo-second order model	$\frac{t}{q_t} = \frac{1}{k_2 q_e^2} + \frac{t}{q_e}$	$\frac{t}{q_t}$ versus time(t)

0.95165 respectively. R^2 values for safranin, malachite green, and mixture at 20 mg nanobiochar dose were 0.95477, 0.79362, and 0.78968 respectively. Overall low R^2 values showed that adsorption kinetics data did not follow the pseudo-first order model (Fig. 11; Table 3).

3.4.2. *Pseudo-second order model*

Pseudo-second order model had been applied to study the adsorption kinetics mechanism. R^2 values for safranin, malachite green, and mixture at 10 mg nanobiochar dose were 0.99793, 0.97251, and 0.97516 respectively. R^2 values for safranin, malachite green, and mixture at 20 mg nanobiochar dose were 0.9991, 0.99977, and 0.97742 respectively. This showed that adsorption kinetics data for both dyes and their mixture followed the pseudo-second order model representing chemisorption (Aoulad et al., 2023) including mechanisms i.e., ion exchange, H bonding, complexation, electrostatic interaction etc (Naseri et al., 2023) (Fig. 12; Table 4).

4. Discussion

Nanobiochar has proved to be a better adsorbent as increase in reactive oxygen species and negative zeta potential, reduction in hydrodynamic radius and increase in C and O containing functional groups have upgraded the adsorptive potential of nanobiochar (Ramanayaka et al., 2020). In current study adsorption of dyes by nanobiochar had been studied by changing certain variables such as temperature, contact time, nanobiochar dose, and pH. Pseudo first order and pseudo second order kinetic models had been applied to study the adsorption kinetics of dyes. The elimination percentages graph had shown that the elimination

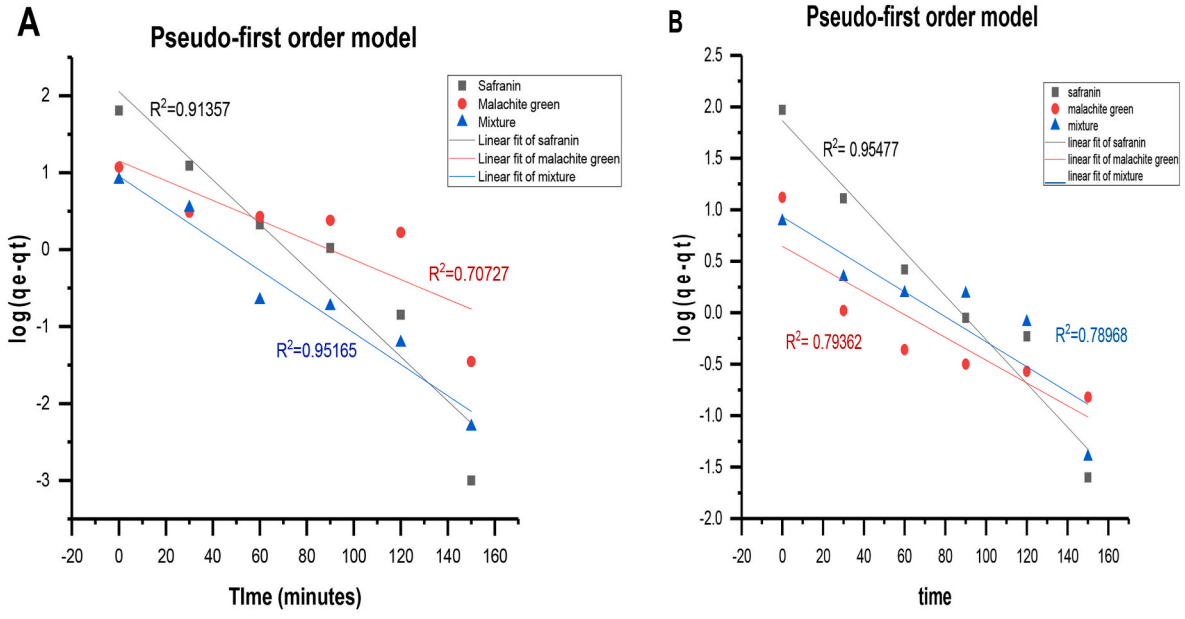

Fig. 11. Pseudo-first order model (A) 10 mg nanobiochar (B) 20 mg nanobiochar.

Table 3
Kinetic parameters of pseudo-first order model for adsorption of dyes.

Pseudo first order model				
Amount of nanobiochar	Parameters	Safranin	Malachite green	Mixed dyes
10 mg nanobiochar	qe (mg/g)	64.015	11.8105	8.066
	K_1 (min^{-1})	−0.02872 ± 0.00442	−0.01284 ± 0.00413	−0.02037 ± 0.0023
	R^2	0.91357	0.70727	0.95165
20 mg nanobiochar	qe (mg/g)	94	13.2	7.716
	K1 (min-1)	−0.02128 ± 0.00232	−0.01106 ± 0.00282	−0.01214 ± 0.00313
	R2	0.95477	0.79362	0.78968

of safranin and malachite green was elevated at a temperature of 50 °C, with high nanobiochar dose, and pH of 7.

Maximum elimination percentages of safranin, malachite green, and a mixture of dyes obtained were 91.7%, 87.5%, and 85% respectively. Numerous adsorbents such as biochar, activated carbon, zeolite, and chitosan are being used for dye removal. Rice husk biochar has been used for the removal of Basic Blue 41 and Basic Red 09 dyes from the aqueous solution with an 80% elimination percentage under optimal conditions (Saravanan et al., 2023). Mesoporous zeolite made from biopolymer chitin has been used for the adsorption of crystal violet (CV), methylene blue (MB), and basic fuchsin (BF) with maximum efficiency of 85% color removal (Brião et al., 2018). Chitosan has been used as an adsorbent of Azo dyes from aqueous solution with 86% maximum removal (Jabbar et al., 2014). The combination of the coagulation-flocculation process and adsorption by activated carbon produced from sludge showed an 85.2% elimination percentage of dyes (Puchana-Rosero et al., 2018). In another study maximum removal capacity of phillipsite for safranin was recorded to be 88% with application of 0.25 g of reported zeolite thus reducing the overall efficiency of adsorbant due to its high dosage required to remove pollutant (Abukhadra and Mohamed, 2019). A adsorption study conducted on removal of malachite green by chitosan reported 86.55% removal by protonated crosslinked chitosan beads following pseudo second order kinetic model (Sadiq et al., 2021). Higher removal efficiency of nanobiochar compared to reported studies can be attributed owing to its large surface area, porosity, total pore volume, and active sites present on nanobiochar.

An increase in adsorption capacity with an increase in temperature has shown the endothermic nature of the adsorption process (Bhattacharyya et al., 2018). The active sites present on nanobiochar and porosity and total pore volume increased with temperature causing an increase in binding of dye molecules to the nanobiochar surface and eventually more adsorption (Bilir et al., 2013; Sun et al., 2013). In majority studies with increasing temperature value, the solubility of the dye decreases, and therefore the adsorption increases (Aoulad et al., 2023). High temperature causes an increase in active sites on adsorbent with along with making it more desolvated. Temperature also positively effects the frequency at which dyes collide with functional groups present on surface of nanobiochar leading to increase in adsorption process. It shows an increase in interaction between dye molecules and biochar active sites and the equilibrium capacity of nanobiochar (Acemioğlu, 2022). Literature has shown that the diffusion rate of dyes to the

Table 4
Kinetic parameters of pseudo-second order model for the adsorption of dyes.

Pseudo- second order model				
Amount of nanobiochar	Parameters	Safranin	Malachite green	Mixed dyes
10 mg nanobiochar	qe (mg/g)	64.015	11.8105	8.066
	k_2 (g mg^{-1} min^{-1})	0.0153 ± 3.48782E-4	0.08752 ± 0.00736	0.1162 ± 0.00927
	R^2	0.99793	0.97251	0.97516
20 mg nanobiochar	qe (mg/g)	94	13.2	7.716
	k_2 (g mg^{-1} min^{-1})	0.01051 ± 1.57837E-4	0.07636 ± 5.73012E-4	0.13169 ± 0.01001
	R^2	0.9991	0.99977	0.97742

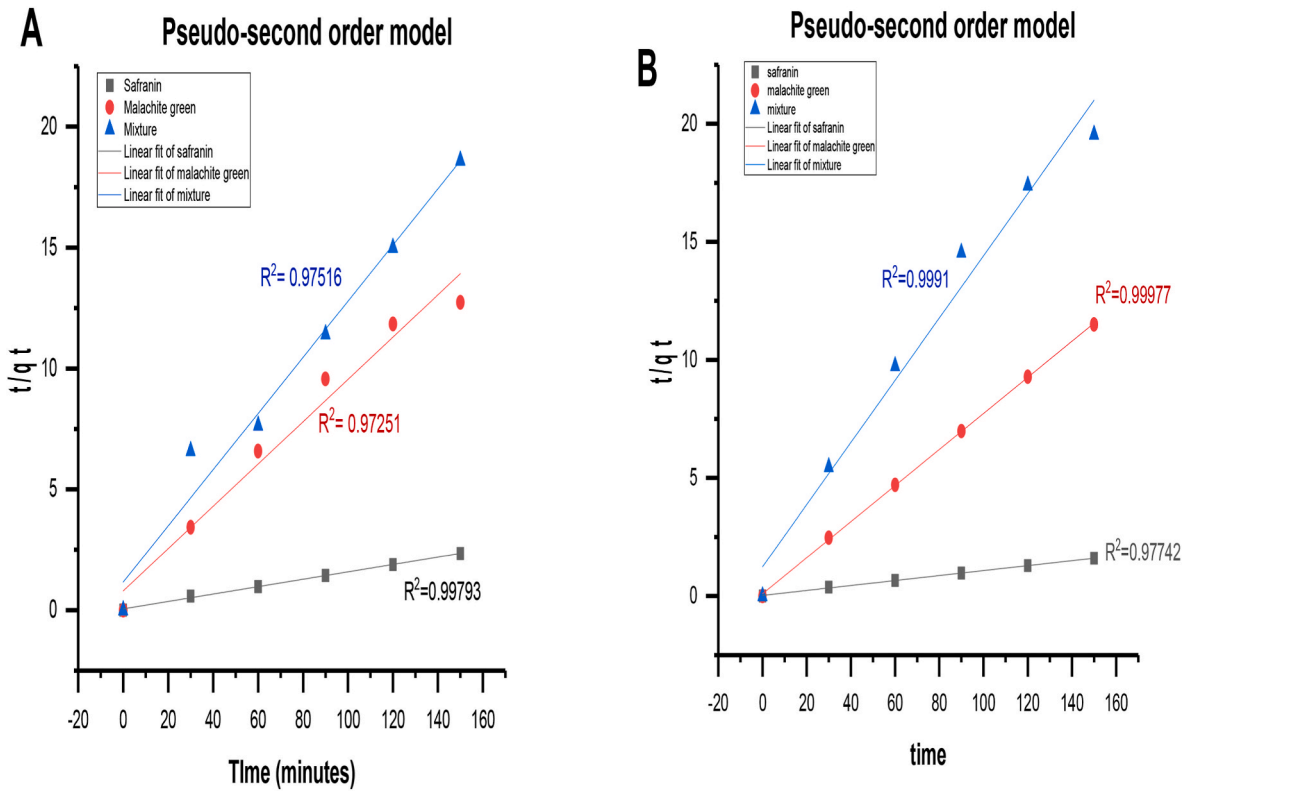

Fig. 12. Pseudo-second order model (A) 10 mg nanobiochar (B) 20 mg nanobiochar.

external surface and internal pores of the nanobiochar particles increases with an increase in temperature and the kinetic energy of dyes molecules increase their mobility to attach to the nanobiochar surface (Behera et al., 2008; Güzel et al., 2015, 2017). Crystal violet and basic fuchsin have also shown similar patterns (Mohan et al., 2002). The adsorption of dyes is correlated with ion exchange due to which capacity of adsorption is influenced by variation in pH (Rafatullah et al., 2010).

By increasing nanobiochar dose, active positions for binding of dyes and surface area for sorption increased which caused an increase in adsorption rate and elimination percentages (Li et al., 2018). It was observed from qt versus t plots that the sorption rate increased sharply within 30 min then it increased slowly until it reaches equilibrium. This outcome is due to the presence of a huge concentration gradient between solution dye and dye in nanobiochar in the initial stage because of plentiful free active sites present on nanobiochar (Güzel et al., 2015). Then, the mass transfer of dyes from the bulk solution to the external surface of nanobiochar and within nanobiochar particles slows down due to fewer vacant sites until the equilibrium stage is reached (Güzel et al., 2015). The mixture of dyes has shown deviation from normal trends due to changes in their behavior by different interactions between them.

In the current study, cationic dyes (malachite green and sfranin) were chosen as the focus of the experiment. The use of acidic pH was not considered since previous studies conducted by (Agarwal et al., 2016; Fayazi et al., 2015; Ishaq et al., 2017; Jalal and Fakhre, 2022) have consistently supported the use of neutral to alkaline pH for the removal of cationic dyes from water. On the other hand, acidic pH has been found to be more favourable for the removal of anionic dyes, such as methyl orange from aqueous solutions, due to the strong interaction between H+ and OH- ions (Aichour et al., 2022).

In another study, a decline in the adsorption of the cationic dye methylene blue was observed as the solution's pH shifted towards acidic conditions. Conversely, moving towards alkaline conditions resulted in an increased adsorption capacity of positively charged dyes, attributed to surface electrostatic attraction due to negative potential effects (Kaya et al., 2018). These findings highlight the importance of considering the pH conditions when dealing with cationic dyes, as the adsorption behavior varies significantly with changes in pH levels. Effect of pH on adsorption of dyes on nanobiochar suggested that both neutral and alkaline pH favours the process with more dye's removal from solution. It can be attributed to number of complex factors as in this study neutral pH favoured removal of safranin and malachite individually however maximum removal for mixture of both dyes was obtained at alkaline pH. For cationic dyes as malachite green and safranin at low or acidic pH, dye is protonated and exits in its cationic form. In addition, many protons available in solution protonate the biochar surface, thus both nanobiocahr and cationic dyes having net positive charges undergoes electrostatic repulsion, decreasing the amount of dye adsorbed on nanobiochar. At higher pH both nanobiochar and dyes develop opposite charges leading to electrostatic attraction between positively charged dyes and negatively charged nanobiochar, resulting in maximum adsorption. Increasing solution pH increases the number of carboxylate anion (COO^-) and hydroxyl groups (OH) on nanobiochar surface thus increasing negatively charged sites. These oxygenated negatively charges sites are available for functional groups of dye to get attached causing maximum removal from solution. Electrostatic interaction is main mechanism for removal of dyes on biochar generated from various substrates (Phuong et al., 2019).

By applying kinetic models, it has been observed that adsorption kinetic data follows the pseudo-second order model representing chemisorption (Aoulad et al., 2023). Chemical adsorption including mechanisms i.e., ion exchange, complexation, electrostatic interaction etc (Naseri et al., 2023; Sahoo and Prelot, 2020). Electrostatic interactions are one of the most common adsorption mechanisms by nanobiochar for removal of organic pollutants (Abbas et al., 2018). In some cases experimental conditions also determine the type of forces involved in adsorption process. In a study with the pH value ranging from 1.8 to 9.8, the adsorption capacity of nanobiochar for methyl blue shifted from 216 to 351 mg/g, indicating that the electrostatic interaction mechanism plays an important role in the adsorption process (Lyu et al., 2018). Functional groups present on the surface of nanobiochar promote the chemical combination of positively charged dye and negatively charged nanobiochar. The adsorption porcess may also include other interactions including hydrogen bonds, π - π stacking, and van der Waals forces (Song et al., 2019).

Dye adsorption onto the nanobiochar surface involves several mechanisms, including ion exchange, complexation, precipitation, electrostatic interaction, and physical adsorption (Jiang et al., 2023). The specific reactions occurring during the adsorption process may vary depending on factors such as nanobiochar properties, environmental conditions, and the type of adsorbed pollutants (Mahmoud et al., 2020a, b).

Studies have shown that the adsorption of certain dyes like Ni on carbonaceous materials mainly involves chemisorption including electrostatic forces, cationic-π interactions, and surface complexation, whereas the adsorption mechanism of glyphosate on nanobiochar may not follow this pattern (Meena et al., 2005; Ramanayaka et al., 2020a,b). High-temperature pyrolysis can result in increased specific surface area (SSA) and void structure richness of biochar, leading to a dominant physical adsorption mechanism. Conversely, low-temperature nanobiochar with relatively lower SSA and higher polar surface functional groups tends to exhibit a dominant chemical adsorption mechanism (Zhuang et al., 2021).

Physical interactions in the adsorption process include pore filling, π stacking, and H-bonding, which are influenced by nanobiochar's surface area, porosity, and aromaticity. Enhanced surface area and pore volume facilitate the diffusion of contaminants, while the aromatic structure of nanobiochar promotes π-stacking and H-bond interactions with pollutants (Inyang et al., 2016). Hydroxyl and amine groups on the nanobiochar surface can also participate in π–π interactions with electron-deficient functional groups present in cationic dyes (Choudhary et al., 2020). Electrostatic interactions are also the most common adsorption mechanism when nanobiochar binds to organic pollutants (Abbas et al., 2018). The strength and nature of the electrostatic force depend on the solution pH. Nanobiochar with graphene structure and larger pore volume and size may experience more frequent pore filling and π–π interactions during the adsorption process (Lyu et al., 2018). In the case of malachite green, adsorption onto litchi biochar was found to follow mechanisms such as pore filling effect, π–π interactions, electrostatic interactions, and hydrogen bonding (Wu et al., 2020).

5. Limitations

Nanobiochar is a relatively new material, and research on its long-term effects and potential risks in water treatment is still limited. More studies are needed to fully understand its behavior, interactions with pollutants, and potential environmental impacts as its efficiency can vary depending on the type of pollutants present and the water composition. In addition, as lab-scale studies may demonstrate the effectiveness of nanobiochar for water treatment, scaling up the production and implementation of nanobiochar-based water treatment systems can present technical and logistical challenges.

Nanobiochar can be an effective additive for pollutant removal not only from water but can also be used for stabilization of pollutants in polluted soils (Jiang et al., 2023). Nanobiochar production from sustainable and low-cost sources i.e., agricultural or any organic waste materials, makes it an eco-friendly and economically viable option for dye removal offering a dual benefit. Along with pollutant removal from water, it also serves as a means of carbon sequestration, effectively trapping carbon in the charred biomass (Wang et al., 2023).

6. Conclusion

The findings of the research indicate that the nanobiochar is an excellent bio adsorbent serving as a prominent solution for removal of dyes from water. The characterization techniques stated that the particles were crystalline and Nano in size. Its crystalline structure and large pore size enhanced the adsorption activity. The yield was 27.5% for biochar and 0.9% for nanobiochar. Nanobiochar exhibited excellent uptake percentages of two dyes. Maximum elimination percentages of safranin, malachite green, and the mixture of dyes were obtained as 91.7%, 87.5%, and 85% respectively. Optimum results were obtained at pH 7, 50 °C temperature, 20 mg nanobiochar, and 30-min contact time. An increase in temperature and nanobiochar dose was found to increase the removal efficiency of safranin, malachite green, and the mixture of both dyes. The adsorption process was found to obey the pseudo-second order kinetic model and indicated a chemical sorption mechanism. By application of nanobiochar derived from rice husk biochar as economically and friendly adsorbents, a noticeable quantity of undesired dyes from industrial effluents can be removed thus offering as a substitute to other expensive adsorbents such as activated carbon or charcoal etc. Technology of nanobiochar provides simultaneous benefits of minimizing rice husk waste into a valuable product to remove dyes from industrial discharges and this technology needs to be scaled up. However the practical application of nanobiochar in environmental settings encounters few obstacles. There are relatively few studies available on nanobiochar. The lack of comprehensive data concerning large-scale synthesis and application of nanobiochar presents challenges in estimating its economic viability. While nanobiochar demonstrates higher adsorption capabilities and improved transportability, there is a need to study biogeochemical behavior of nanobiochar in different ecosystems. To ensure responsible and sustainable usage, thorough investigations into process optimization, eco-toxicity, and life cycle evaluation of nanobiochar fabrication must be conducted before considering commercial-scale synthesis. The optimization of process parameter for desirable properties (porosity, surface area and functionality and binding sites) and yield is required.

CRediT authorship contribution statement

Sadia Aziz: Methodology, Formal analysis, Investigation, Writing – original draft. **Bushra Uzair:** Conceptualization, Software, Resources, Data curation, Writing – original draft, Writing – review & editing, Supervision, Project administration. **Muhammad Ishtiaq Ali:** Methodology and Investigation. **Sundas Ambreen:** Methodology, Investigation. **Fatiha Umber:** Methodology, Investigation. **Muneeba Khalid:** Methodology, Investigation. **Alaa AA. Aljabali:** Validation, Writing – original draft, Writing – review & editing. **Yachana Mishra:** Validation, Writing – original draft, Writing – review & editing. **Vijay Mishra:** Validation, Writing – original draft, Writing – review & editing. **Ángel Serrano-Aroca:** Validation, Writing – original draft, Writing – review & editing. **Gowhar A. Naikoo:** Validation, Writing – original draft, Writing – review & editing. **Mohamed El-Tanani:** Writing – original draft, Writing – review & editing. **Shafiul Haque:** Writing – review & editing. **Abdulmajeed G. Almutary:** Writing – review & editing. **Murtaza M. Tambuwala:** Conceptualization, Software, Resources, Writing – review & editing, Supervision, Project administration.

Declaration of competing interest

The authors declare that they have no known competing financial interests or personal relationships that could have appeared to influence the work reported in this paper.

Data availability

Data will be made available on request.

Acknowledgements

Funded and supported by International Islamic University, Islamabad, Pakistan.

References

Aarimuthu, G., Sathiasivan, K., Varadharajan, S., Balakrishnan, M., Albeshr, M.F., Alrefaei, A.F., Kim, W., 2023. Enhanced membraneless fuel cells by electrooxidation of ethylene glycol with a nanostructured cobalt metal catalyst. Environ. Res. 233 (March), 115601 https://doi.org/10.1016/j.envres.2023.115601.

Abbas, Z., Ali, S., Rizwan, M., Zaheer, I.E., Malik, A., Riaz, M.A., Shahid, M.R., Rehman, M. Z. ur, Al-Wabel, M.I., 2018. A critical review of mechanisms involved in the adsorption of organic and inorganic contaminants through biochar. Arabian J. Geosci. 11 (16) https://doi.org/10.1007/s12517-018-3790-1.

Abukhadra, M.R., Mohamed, A.S., 2019. Adsorption removal of safranin dye contaminants from water using various types of natural zeolite. Silicon 11 (3), 1635–1647. https://doi.org/10.1007/s12633-018-9980-3.

Acemioğlu, B., 2022. Removal of a reactive dye using NaOH-activated biochar prepared from peanut shell by pyrolysis process. Int. J. Coal Preparation Util. 42 (3), 671–693. https://doi.org/10.1080/19392699.2019.1644326.

Agarwal, S., Tyagi, I., Gupta, V.K., Mashhadi, S., Ghasemi, M., 2016. Kinetics and thermodynamics of Malachite Green dye removal from aqueous phase using iron nanoparticles loaded on ash. J. Mol. Liq. 223, 1340–1347. https://doi.org/10.1016/j.molliq.2016.04.039.

Aichour, A., Zaghouane-Boudiaf, H., Djafer Khodja, H., 2022. Highly removal of anionic dye from aqueous medium using a promising biochar derived from date palm petioles: characterization, adsorption properties and reuse studies. Arab. J. Chem. 15 (1), 103542 https://doi.org/10.1016/j.arabjc.2021.103542.

Amen, R., Yaseen, M., Mukhtar, A., Klemeš, J.J., Saqib, S., Ullah, S., Bokhari, A., 2020. Lead and cadmium removal from wastewater using eco-friendly biochar adsorbent derived from rice husk, wheat straw, and corncob. Cleaner Eng. Tech. 1, 100006 https://doi.org/10.1016/j.clet.2020.100006.

Anupama, Khare, P., 2021. A comprehensive evaluation of inherent properties and applications of nano-biochar prepared from different methods and feedstocks. J. Clean. Prod. 320 (January), 128759 https://doi.org/10.1016/j.jclepro.2021.128759.

Aoulad, Y., Hadj, E., Mohammadi, A., Ait, A., Youness, L., 2023. Recent advances and prospects of biochar - based adsorbents for malachite green removal : a comprehensive review. Chem. Africa 6 (2), 579–608. https://doi.org/10.1007/s42250-022-00391-8.

Behera, S.K., Kim, J.-H., Guo, X., Park, H.-S., 2008. Adsorption equilibrium and kinetics of polyvinyl alcohol from aqueous solution on powdered activated carbon. J. Hazard Mater. 153 (3), 1207–1214. https://doi.org/10.1016/j.jhazmat.2007.09.117.

Benkhaya, S., M'rabet, S., El Harfi, A., 2020. A review on classifications, recent synthesis and applications of textile dyes. Inorg. Chem. Commun. 115, 107891.

Bhattacharyya, A., Banerjee, B., Ghorai, S., Rana, D., Roy, I., Sarkar, G., Saha, N.R., De, S., Ghosh, T.K., Sadhukhan, S., Chattopadhyay, D., 2018. Development of an auto-phase separable and reusable graphene oxide-potato starch based cross-linked bio-composite adsorbent for removal of methylene blue dye. Int. J. Biol. Macromolecules 116, 1037–1048. https://doi.org/10.1016/j.ijbiomac.2018.05.069.

Bilir, M.H., Sakalar, N., Acemioglu, B., Baran, E., Alma, M.H., 2013. Sorption of remazol brilliant blue R onto polyurethane-type foam prepared from peanut shell. J. Appl. Polym. Sci. 127 (6), 4340–4351. https://doi.org/10.1002/app.37614.

Brião, G.V., Jahn, S.L., Foletto, E.L., Dotto, G.L., 2018. Highly efficient and reusable mesoporous zeolite synthetized from a biopolymer for cationic dyes adsorption. Colloids Surf. A Physicochem. Eng. Asp. 556, 43–50. https://doi.org/10.1016/j.colsurfa.2018.08.019.

Bushra, B., Remya, N., 2020. Biochar from pyrolysis of rice husk biomass—characteristics, modification and environmental application. Biomass Conv. Biorefinery. https://doi.org/10.1007/s13399-020-01092-3.

Cantrell, K.B., Hunt, P.G., Uchimiya, M., Novak, J.M., Ro, K.S., 2012. Impact of pyrolysis temperature and manure source on physicochemical characteristics of biochar. Bioresour. Technol. 107, 419–428. https://doi.org/10.1016/j.biortech.2011.11.084.

Chauhan, P., Imam, A., Kanaujia, P.K., Suman, S.K., 2023. Nano-bioremediation: an eco-friendly and effective step towards petroleum hydrocarbon removal from environment. Environ. Res. 231 (P2), 116224 https://doi.org/10.1016/j.envres.2023.116224.

Chen, Z., Pei, J., Wei, Z., Ruan, X., Hua, Y., Xu, W., Guo, Y., 2021. A novel maize biochar-based compound fertilizer for immobilizing cadmium and improving soil quality and maize growth. Environ. Pollut. 277, 116455 https://doi.org/10.1016/j.envpol.2021.116455.

Choudhary, M., Kumar, R., Neogi, S., 2020. Activated biochar derived from Opuntia ficus-indica for the efficient adsorption of malachite green dye, Cu+2 and Ni+2 from water. J. Hazard Mater. 392 (February), 122441 https://doi.org/10.1016/j.jhazmat.2020.122441.

Claoston, N., Samsuri, A.W., Ahmad Husni, M.H., Mohd Amran, M.S., 2014. Effects of pyrolysis temperature on the physicochemical properties of empty fruit bunch and rice husk biochars. Waste Manag. Res. 32 (4), 331–339. https://doi.org/10.1177/0734242X14525822.

Eltaweil, A., Mohamed, H.A., Abd El-Monaem, E.M., El-Subruiti, G., 2020. Mesoporous magnetic biochar composite for enhanced adsorption of malachite green dye: characterization, adsorption kinetics, thermodynamics and isotherms. Adv. Powder Technol. 31 (3), 1253–1263.

Fayazi, M., Afzali, D., Taher, M.A., Mostafavi, A., Gupta, V.K., 2015. Removal of Safranin dye from aqueous solution using magnetic mesoporous clay: optimization study. J. Mol. Liq. 212, 675–685. https://doi.org/10.1016/j.molliq.2015.09.045.

Goswami, L., Kushwaha, A., Singh, A., Saha, P., Choi, Y., Maharana, M., Patil, S.V., Kim, B.S., 2022. Nano-biochar as a sustainable catalyst for anaerobic digestion: a synergetic closed-loop approach. Catalysts 12 (2), 1–23. https://doi.org/10.3390/catal12020186.

Güzel, F., Sayğılı, H., Akkaya Sayğılı, G., Koyuncu, F., 2015. New low-cost nanoporous carbonaceous adsorbent developed from carob (Ceratonia siliqua) processing industry waste for the adsorption of anionic textile dye: characterization, equilibrium and kinetic modeling. J. Mol. Liq. 206, 244–255. https://doi.org/10.1016/j.molliq.2015.02.037.

Güzel, F., Sayğılı, H., Akkaya Sayğılı, G., Koyuncu, F., Yılmaz, C., 2017. Optimal oxidation with nitric acid of biochar derived from pyrolysis of weeds and its application in removal of hazardous dye methylene blue from aqueous solution. J. Clean. Prod. 144, 260–265. https://doi.org/10.1016/j.jclepro.2017.01.029.

Heidarinejad, Z., Dehghani, M.H., Heidari, M., Javedan, G., Ali, I., Sillanpää, M., 2020. Methods for preparation and activation of activated carbon: a review. Environ. Chem. Lett. 18 (2), 393–415. https://doi.org/10.1007/s10311-019-00955-0.

Heshammuddin, N.A., Al-Gheethi, A., Saphira Radin Mohamed, R.M., Bin Khamidun, M. H., 2023. Eliminating xenobiotics organic compounds from greywater through green synthetic nanoparticles. Environ. Res. 222 (November 2022), 115316 https://doi.org/10.1016/j.envres.2023.115316.

Inyang, M.I., Gao, B., Yao, Y., Xue, Y., Zimmerman, A., Mosa, A., Pullammanappallil, P., Ok, Y.S., Cao, X., 2016. A review of biochar as a low-cost adsorbent for aqueous heavy metal removal. Crit. Rev. Environ. Sci. Technol. 46 (4), 406–433. https://doi.org/10.1080/10643389.2015.1096880.

Ishaq, M., Sultan, S., Ahmad, I., Saeed, K., 2017. Removal of brilliant green dye from aqueous medium by untreated acid treated and magnetite impregnated bentonite adsorbents. J. Chem. Soc. Pakistan 39 (5), 780–787.

Jabbar, Z., Angham, A., Sami, G.J.O., 2014. Removal of azo dye from aqueous solutions using chitosan. Orient. J. Chem. 30 (2), 571–575.

Jalal, A.F., Fakhre, N.A., 2022. Removal of dyes (BG, MG, and SA) from aqueous solution using a novel adsorbent macrocyclic compound. PLoS One 17 (10 October), 1–20. https://doi.org/10.1371/journal.pone.0275330.

Jiang, M., He, L., Niazi, N.K., Wang, H., Gustave, W., Vithanage, M., Geng, K., Shang, H., Zhang, X., Wang, Z., 2023. Nanobiochar for the remediation of contaminated soil and water: challenges and opportunities. Biochar 5 (1). https://doi.org/10.1007/s42773-022-00201-x.

Karimi-Maleh, H., Darabi, R., Baghayeri, M., Karimi, F., Fu, L., Rouhi, J., Niculina, D.E., Gündüz, E.S., Dragoi, E.N., 2023. Recent developments in carbon nanomaterials-based electrochemical sensors for methyl parathion detection. J. Food Meas. Char. https://doi.org/10.1007/s11694-023-02050-z.

Kaya, N., Yıldız, Z., Ceylan, S., 2018. Preparation and characterisation of biochar from hazelnut shell and its adsorption properties for methylene blue dye. J. Polytech. 0900 (4), 765–776. https://doi.org/10.2339/politeknik.386963.

Le, P.T., Bui, H.T., Le, D.N., Nguyen, T.H., Pham, L.A., Nguyen, H.N., Nguyen, Q.S., Nguyen, T.P., Bich, N.T., Duong, T.T., Herrmann, M., Ouillon, S., Le, T.P.Q., 2021. Preparation and characterization of biochar derived from agricultural by-products for dye removal. Adsorpt. Sci. Technol. 2021 https://doi.org/10.1155/2021/9161904.

Li, B., Wang, Q., Guo, J.-Z., Huan, W.-W., Liu, L., 2018. Sorption of methyl orange from aqueous solution by protonated amine modified hydrochar. Bioresour. Technol. 268, 454–459. https://doi.org/10.1016/j.biortech.2018.08.023.

Liu, G., Zheng, H., Jiang, Z., Zhao, J., Wang, Z., Pan, B., Xing, B., 2018. Formation and physicochemical characteristics of nano biochar: insight into chemical and colloidal stability. Environ. Sci. Technol. 52 (18), 10369–10379. https://doi.org/10.1021/acs.est.8b01481.

Liu, H., Hu, M., Zhang, H., Wei, J., 2022. Biosynthesis of stalk Biochar-nZVI and its catalytic reactivity in degradation of dyes by persulfate. Surface. Interfac. 31 (April), 102098 https://doi.org/10.1016/j.surfin.2022.102098.

Lyu, H., Gao, B., He, F., Zimmerman, A.R., Ding, C., Tang, J., Crittenden, J.C., 2018. Experimental and modeling investigations of ball-milled biochar for the removal of aqueous methylene blue. Chem. Eng. J. 335, 110–119. https://doi.org/10.1016/j.cej.2017.10.130.

Ma, S., Jing, F., Sohi, S.P., Chen, J., 2019. New insights into contrasting mechanisms for PAE adsorption on millimeter, micron- and nano-scale biochar. Environ. Sci. Pollut. Control Ser. 26 (18), 18636–18650. https://doi.org/10.1007/s11356-019-05181-3.

Mahmoud, M.E., El-Ghanam, A.M., Saad, S.R., Mohamed, R.H.A., 2020a. Promoted removal of metformin hydrochloride anti-diabetic drug from water by fabricated and modified nanobiochar from artichoke leaves. Sustain. Chem. Pharmac. 18 (July), 100336 https://doi.org/10.1016/j.scp.2020.100336.

Mahmoud, M.E., Abdelfattah, A.M., Tharwat, R.M., Nabil, G.M., 2020b. Adsorption of negatively charged food tartrazine and sunset yellow dyes onto positively charged triethylenetetramine biochar: optimization, kinetics and thermodynamic study. J. Mol. Liq. 318, 114297 https://doi.org/10.1016/j.molliq.2020.114297.

Meena, A.K., Mishra, G.K., Rai, P.K., Rajagopal, C., Nagar, P.N., 2005. Removal of heavy metal ions from aqueous solutions using carbon aerogel as an adsorbent. J. Hazard Mater. 122 (1–2), 161–170. https://doi.org/10.1016/j.jhazmat.2005.03.024.

Mohammed, Z., Jeelani, S., Rangari, V., 2021. Low temperature plasma treatment of rice husk derived hybrid silica/carbon biochar using different gas sources. Mater. Lett. 292, 129678 https://doi.org/10.1016/j.matlet.2021.129678.

Mohan, D., Singh, K.P., Singh, G., Kumar, K., 2002. Removal of dyes from wastewater using flyash, a low-cost adsorbent. Ind. Eng. Chem. Res. 41 (15), 3688–3695. https://doi.org/10.1021/ie010667+.

Monica Nwajiaku, I., Sato, K., Tokunari, T., Kitano, S., Masunaga, T., 2018. Improvement of rice husk residue silicon availability for replenishing available silicon in paddy soil. Int. J. Phys. Soc. Sci. 24 (2), 1–11. https://doi.org/10.9734/IJPSS/2018/43220.

Morales, L.F., Herrera, K., López, J.E., Saldarriaga, J.F., 2021. Use of biochar from rice husk pyrolysis: assessment of reactivity in lime pastes. Heliyon 7 (11), e08423. https://doi.org/10.1016/j.heliyon.2021.e08423.

Naseri, A., Abed, Z., Rajabi, M., Lal, B., Asghari, A., Baigenzhenov, O., Arghavani-Beydokhti, S., Hosseini-Bandegharaei, A., 2023. Use of Chrysosporium/carbon nanotubes for preconcentration of ultra-trace cadmium levels from various samples after extensive studies on its adsorption properties. Chemosphere 335 (June), 139168. https://doi.org/10.1016/j.chemosphere.2023.139168.

Ng, L.Y.F., Ariffin, H., Yasim-Anuar, T.A.T., Farid, M.A.A., Hassan, M.A., 2022. High-energy ball milling for high productivity of nanobiochar from oil palm biomass. Nanomaterials 12 (18), 1–11. https://doi.org/10.3390/nano12183251.

Noreen, S., Abd-Elsalam, K.A., 2021. Chapter 9 - biochar-based nanocomposites: a sustainable tool in wastewater bioremediation. In: Abd-Elsalam, K.A., Zahid, M. (Eds.), Aquananotechnology. Elsevier, pp. 185–200. https://doi.org/10.1016/B978-0-12-821141-0.00023-9.

Novak, J.M., Busscher, W.J., Laird, D.L., Ahmedna, M., Watts, D.W., Niandou, M.A.S., 2009. Impact of biochar amendment on fertility of a southeastern coastal plain soil. Soil Sci. 174 (2), 105–112. https://doi.org/10.1097/SS.0b013e3181981d9a.

Nwajiaku, I.M., Olanrewaju, J.S., Sato, K., Tokunari, T., Kitano, S., Masunaga, T., 2018. Change in nutrient composition of biochar from rice husk and sugarcane bagasse at varying pyrolytic temperatures. Int. J. Recycl. Org. Waste Agric. 7 (4), 269–276. https://doi.org/10.1007/s40093-018-0213-y.

Oliveira, M.G., Spaolonzi, M.P., Duarte, E.D.V., Costa, H.P.S., da Silva, M.G.C., Vieira, M. G.A., 2023. Adsorption kinetics of ciprofloxacin and ofloxacin by green-modified carbon nanotubes. Environ. Res. 233 (June), 116503 https://doi.org/10.1016/j.envres.2023.116503.

Pan, X., Gu, Z., Chen, W., Li, Q., 2021. Preparation of biochar and biochar composites and their application in a Fenton-like process for wastewater decontamination: a review. Sci. Total Environ. 754, 142104.

Phuong, D.T.M., Loc, N.X., Miyanishi, T., 2019. Efficiency of dye adsorption by biochars produced from residues of two rice varieties, Japanese Koshihikari and Vietnamese IR50404. Desalination Water Treat. 165, 333–351. https://doi.org/10.5004/dwt.2019.24496.

Pottmaier, D., Costa, M., Farrow, T., Oliveira, A.A.M., Alarcon, O., Snape, C., 2013. Comparison of rice husk and wheat straw: from slow and fast pyrolysis to char combustion. Energy Fuels 27 (11), 7115–7125. https://doi.org/10.1021/ef401748e.

Puchana-Rosero, M.J., Lima, E.C., Mella, B., Costa, D.d., Poll, E., Gutterres, M.J.J., 2018. A coagulation-flocculation process combined with adsorption using activated carbon obtained from sludge for dye removal from tannery wastewater. J. Chil. Chem. Soc. 63 (1), 3867–3874.

Qian, L., Zhang, W., Yan, J., Han, L., Gao, W., Liu, R., Chen, M., 2016. Effective removal of heavy metal by biochar colloids under different pyrolysis temperatures. Bioresour. Technol. 206, 217–224. https://doi.org/10.1016/j.biortech.2016.01.065.

Rafatullah, M., Sulaiman, O., Hashim, R., Ahmad, A., 2010. Adsorption of methylene blue on low-cost adsorbents: a review. J. Hazard Mater. 177 (1), 70–80. https://doi.org/10.1016/j.jhazmat.2009.12.047.

Rajput, V.D., Minkina, T., Ahmed, B., Singh, V.K., Mandzhieva, S., Sushkova, S., Wang, B., 2022. Nano-biochar: a novel solution for sustainable agriculture and environmental remediation. Environ. Res. 210, 112891 https://doi.org/10.1016/j.envres.2022.112891.

Ramanayaka, S., Vithanage, M., Alessi, D.S., Liu, W.J., Jayasundera, A.C.A., Ok, Y.S., 2020a. Nanobiochar: production, properties, and multifunctional applications. Environ. Sci.: Nano 7 (11), 3279–3302. https://doi.org/10.1039/d0en00486c.

Ramanayaka, S., Tsang, D.C.W., Hou, D., Ok, Y.S., Vithanage, M., 2020b. Green synthesis of graphitic nanobiochar for the removal of emerging contaminants in aqueous media. Sci. Total Environ. 706, 135725 https://doi.org/10.1016/j.scitotenv.2019.135725.

Ramasundaram, S., Manikandan, V., Vijayalakshmi, P., Devanesan, S., Salah, M. Bin, Ramesh Babu, A.C., Priyadharsan, A., Oh, T.H., Ragupathy, S., 2023. Synthesis and investigation on synergetic effect of activated carbon loaded silver nanoparticles with enhanced photocatalytic and antibacterial activities. Environ. Res. 233, 1–17. https://doi.org/10.1016/j.envres.2023.116431.

Saadh, M.J., Baher, H., Li, Y., chaitanya, M., Arias-Gonzáles, J.L., Allela, O.Q.B., Mahdi, M.H., Carlos Cotrina-Aliaga, J., Lakshmaiya, N., Ahjel, S., Amin, A.H., Gilmer Rosales Rojas, G., Ameen, F., Ahsan, M., Akhavan-Sigari, R., 2023. The bioengineered and multifunctional nanoparticles in pancreatic cancer therapy: bioresponsive nanostructures, phototherapy and targeted drug delivery. Environ. Res. 233 (June), 116490 https://doi.org/10.1016/j.envres.2023.116490.

Sadiq, A.C., Olasupo, A., Rahim, N.Y., Ngah, W.S.W., Suah, F.B.M., 2021. Comparative removal of malachite green dye from aqueous solution using deep eutectic solvents modified magnetic chitosan nanoparticles and modified protonated chitosan beads. J. Environ. Chem. Eng. 9 (5), 106281 https://doi.org/10.1016/j.jece.2021.106281.

Sahoo, T.R., Prelot, B., 2020. Chapter 7 - adsorption processes for the removal of contaminants from wastewater: the perspective role of nanomaterials and nanotechnology. In: Bonelli, B., Freyria, F.S., Rossetti, I., Sethi, R. (Eds.), Nanomaterials for the Detection and Removal of Wastewater Pollutants. Elsevier, pp. 161–222. https://doi.org/10.1016/B978-0-12-818489-9.00007-4.

Saravanan, P., Josephraj, J., Thillainayagam, B.P., Ravindiran, G., 2023. Evaluation of the adsorptive removal of cationic dyes by greening biochar derived from agricultural bio-waste of rice husk. Biomass Conver. Bioref. 13 (5), 4047–4060. https://doi.org/10.1007/s13399-021-01415-y.

Sarkar, A., Ranjan, A., Paul, B., 2019. Synthesis, characterization and application of surface-modified biochar synthesized from rice husk, an agro-industrial waste for the

removal of hexavalent chromium from drinking water at near-neutral pH. Clean Technol. Environ. Policy 21 (2), 447–462.
Singh, B., Mm, D., Shen, Q., Camps Arbestain, M., 2017. Chapter 3. Biochar pH, electrical conductivity and liming potential, pp. 23–38.
Song, B., Chen, M., Zhao, L., Qiu, H., Cao, X., 2019. Physicochemical property and colloidal stability of micron- and nano-particle biochar derived from a variety of feedstock sources. Sci. Total Environ. 661, 685–695. https://doi.org/10.1016/j.scitotenv.2019.01.193.
Subramanian, H., Santhaseelan, H., Dinakaran, V.T., Devendiran, V., Rathinam, A.J., Mahalingam, A., Ramachandran, S.K., Muthukumarasamy, A., Muthukumar, K., Mathimani, T., 2023. Hydrothermal synthesis of spindle structure copper ferrite-graphene oxide nanocomposites for enhanced photocatalytic dye degradation and in-vitro antibacterial activity. Environ. Res. 231 (P2), 116095 https://doi.org/10.1016/j.envres.2023.116095.
Sun, L., Wan, S., Luo, W., 2013. Biochars prepared from anaerobic digestion residue, palm bark, and eucalyptus for adsorption of cationic methylene blue dye: characterization, equilibrium, and kinetic studies. Bioresour. Technol. 140, 406–413. https://doi.org/10.1016/j.biortech.2013.04.116.
Syed, S.S., Jacob, L., Bharath, G., Haija, M.A., Kaushik, A., Banat, F., 2023. Rapid biosynthesis and characterization of metallic gold nanoparticles by olea europea and their potential application in photoelectrocatalytic reduction of 4-nitrophenol. Environ. Res. 222 (September 2022), 115280 https://doi.org/10.1016/j.envres.2023.115280.
Vieira, F.R., Romero Luna, C.M., Arce, G.L.A.F., Ávila, I., 2020. Optimization of slow pyrolysis process parameters using a fixed bed reactor for biochar yield from rice husk. Biomass Bioenergy 132, 105412. https://doi.org/10.1016/j.biombioe.2019.105412.
Vigneshwaran, S., Sirajudheen, P., Karthikeyan, P., Meenakshi, S., 2021. Fabrication of sulfur-doped biochar derived from tapioca peel waste with superior adsorption performance for the removal of Malachite green and Rhodamine B dyes. Surface. Interfac. 23, 100920.
Vishnu, D., Dhandapani, B., Vaishnavi, G., Preethi, V., 2022. Synthesis of tri-metallic surface engineered nanobiochar from cynodon dactylon residues in a single step-Batch and column studies for the removal of copper and lead ions. Chemosphere 286, 131572.
Wang, Z., Dai, L., Yao, J., Guo, T., Hrynsphan, D., Tatsiana, S., Chen, J., 2021. Enhanced adsorption and reduction performance of nitrate by Fe–Pd–Fe3O4 embedded multi-walled carbon nanotubes. Chemosphere 281 (November 2020), 130718. https://doi.org/10.1016/j.chemosphere.2021.130718.
Wang, Z., Hu, L., Zhao, M., Dai, L., Hrynsphan, D., Tatsiana, S., Chen, J., 2022a. Bamboo charcoal fused with polyurethane foam for efficiently removing organic solvents from wastewater: experimental and simulation. Biochar 4 (1), 1–16. https://doi.org/10.1007/s42773-022-00153-2.
Wang, J., Li, W., Zhao, Z., Musoke, F.S.N., Wu, X., 2022b. Ultrasonic activated biochar and its removal of harmful substances in environment. Microorganisms 10 (8). https://doi.org/10.3390/microorganisms10081593.
Wang, L., Deng, J., Yang, X., Hou, R., Hou, D., 2023. Role of biochar toward carbon neutrality. Carbon Res. 2 (1) https://doi.org/10.1007/s44246-023-00035-7.
Weber, K., Quicker, P., 2018. Properties of biochar. Fuel 217 (December 2017), 240–261. https://doi.org/10.1016/j.fuel.2017.12.054.
Wu, J., Yang, J., Feng, P., Huang, G., Xu, C., Lin, B., 2020. High-efficiency removal of dyes from wastewater by fully recycling litchi peel biochar. Chemosphere 246, 125734. https://doi.org/10.1016/j.chemosphere.2019.125734.
Yang, X., Zhang, S., Ju, M., Liu, L., 2019. Preparation and modification of biochar materials and their application in soil remediation. Appl. Sci. 9 (7) https://doi.org/10.3390/app9071365.
Yuan, Y., Zhang, N., Hu, X., 2020a. Effects of wet and dry ball milling on the physicochemical properties of sawdust derived-biochar. Instrum. Sci. Technol. 48 (3), 287–300. https://doi.org/10.1080/10739149.2019.1708751.
Yuan, H., Chen, L., Cao, Z., Hong, F.F., 2020b. Enhanced decolourization efficiency of textile dye Reactive Blue 19 in a horizontal rotating reactor using strips of BNC-immobilized laccase: optimization of conditions and comparison of decolourization efficiency. Biochem. Eng. J. 156, 107501.
Yue, L., Lian, F., Han, Y., Bao, Q., Wang, Z., Xing, B., 2019. The effect of biochar nanoparticles on rice plant growth and the uptake of heavy metals: implications for agronomic benefits and potential risk. Sci. Total Environ. 656, 9–18. https://doi.org/10.1016/j.scitotenv.2018.11.364.
Zhang, Q., Zhang, D., Lu, W., Khan, M.U., Xu, H., Yi, W., Lei, H., Huo, E., Qian, M., Zhao, Y., Zou, R., 2020. Production of high-density polyethylene biocomposites from rice husk biochar: effects of varying pyrolysis temperature. Sci. Total Environ. 738, 1–26. https://doi.org/10.1016/j.scitotenv.2020.139910.
Zhao, F., Shan, R., Li, W., Zhang, Y., Yuan, H., Chen, Y., 2021. Synthesis, characterization, and dye removal of ZnCl2-modified biochar derived from pulp and paper sludge. ACS Omega 6 (50), 34712–34723. https://doi.org/10.1021/acsomega.1c05142.
Zhuang, Z., Wang, L., Tang, J., 2021. Efficient removal of volatile organic compound by ball-milled biochars from different preparing conditions. J. Hazard Mater. 406 https://doi.org/10.1016/j.jhazmat.2020.124676.